

# Mixing and Segregation of two Particulate Solids in the Transverse Plane of a Rotary Kiln

Sumudu Karunarathne<sup>1</sup> Chameera Jayarathna<sup>2</sup> Lars-Andre Tokheim<sup>1</sup>

<sup>1</sup>Department of Process, Energy and Environmental Technology, University College of Southeast Norway, Norway

{sumudu.karunarathne, lars.a.tokheim}@usn.no

<sup>2</sup>Tel-Tek, Norway, chameera.jayarathna@tel-tek.no

## Abstract

Mixing of two granular phases in a rotary kiln was investigated through CFD simulations using a two-dimensional transverse plane based on the Eulerian approach and the kinetic theory of granular flows. Simulations were performed transverse with the aim to investigate mixing of two particulate solids, CaCO<sub>3</sub> and Al<sub>2</sub>O<sub>3</sub>, under the rolling mode. Simulation results indicated particle segregation rather than mixing during the plane rotation. Volume fractions and velocity contours of each phase were examined to understand the mixing and segregation. Particles with lower density and small particle diameter are collected in the middle section of the bed, while particles with a higher density and larger particle diameter get collected at the bottom of the rotating cylinder. Variations in densities and particle sizes of solid particles were identified as the main causes of the particle segregation. Further studies are required to examine the effect of degree of filling on mixing performance and how the use of lifters may improve the mixing efficiency.

*Keywords: rotary kiln, granular flow, rolling mode, active layer, passive layer*

## 1 Introduction

In industry, materials are needed to be processed in various ways to gain the desired quality of the product. Rotary kilns are widely accepted for the pyroprocessing of many types of materials in different industries owing to efficient mixing and heat transfer performances (Liu et al., 2016). Understanding of particles mixing inside the kiln is vital to enhance heat transfer performance within the bed that improvise material conversion rates in pyro processing.

Granular flows of a transverse plane in a rotary kiln can be categorized into six transport modes; slipping, slumping, rolling, cascading, cataracting and centrifuging. Bed motion depends on Froude number, filling degree, wall friction coefficient, ratio of particle to cylinder diameter, angle of internal friction and dynamic angles of repose (Yin et al., 2014). In industrial rotating drums, the rolling or cascading mode is often applied, and the rolling mode is considered optimum for mixing (Demagh et al., 2012; Boateng et al., 2008).

The approach of numerical analysis in multiphase granular flows facilitates understanding of the bed behavior in rotary kilns. CFD simulations can be performed to investigate motions of particles in the bed according to two mathematical models. Both Euler-Lagrange and Euler-Euler models, along with the kinetic theory of granular flow, are used to simulate the bed motion. In the Euler-Lagrange model, the gas phase is treated as a continuum while the solid particles are considered as a discrete phase (Crowe et al., 1998). Trajectories of individual solid particles are calculated to understand the behavior of the kiln bed. The Euler-Euler model considers each phase as a continuum, and continuity and momentum equations for each phase are applied (Valle, 2012).

Both two-dimensional (2D) and three-dimensional (3D) CFD simulations to investigate mixing of one granular phase in a rotary kiln have been reported in the literature. 2D-CFD simulations were done by Liu et al. (2016) to study particle motion and heat transfer in a rotary kiln. The surface particle motion in rotary cylinder was analyzed via a 2D-CFD model to analyze the dynamic characteristics and rheology of a granular viscous flow in a rotary cylinder to validate real cement rotary kiln (Demagh et al., 2012). A three-dimensional study was done by Yin et al. (2014) to understand granular motion during rolling mode in a rotary kiln. The particle residence time and angle of inclination of the rotary kiln were considered in the simulation.

This study focuses on 2D numerical simulations of mixing of two granular phases in a rotating cylinder. Particle motion in a rotating cylinder was considered similar to the bed behavior of the transverse plane in a rotary kiln. The mixing behavior was analyzed considering two granular particle types, of calcium carbonate (CaCO<sub>3</sub>) and aluminum oxide (Al<sub>2</sub>O<sub>3</sub>), in rolling mode. A mathematical model based on the Euler-Euler approach and the kinetic theory of granular flow were used to describe the dynamics of particles in the transverse plane. The behavior of CaCO<sub>3</sub> and Al<sub>2</sub>O<sub>3</sub> was first studied separately, and then mixing of CaCO<sub>3</sub> and Al<sub>2</sub>O<sub>3</sub> was investigated.

CFD simulations were carried out using ANSYS FLUENT 16.2 and 2D model was developed using ANSYS DesignModeler. The model has the geometrical characteristics of a transverse plane of a rotary kiln.

## 2 Model Description

### 2.1 Particle Mixing in a Transverse Plane

The dynamics of the particle bed in a rotating cylinder under rolling mode has been observed by different techniques (Yin et al., 2014). In rolling mode, particles at the top surface of the bed move down continuously while the bottom part moves up showing a plug flow motion. The maximum particle mixing is achieved under rolling mode. Considering the characteristics of the particles movement, the bed motion can be further divided into two regions, an active layer and a passive layer (Boateng et al., 2008). Figure 1 shows a schematic diagram of a kiln operated in rolling mode.

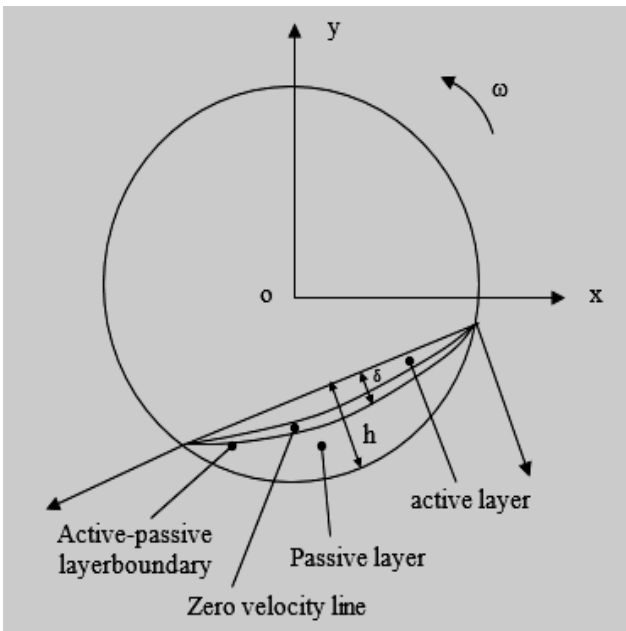


**Figure 1.** Schematic diagram of a kiln operated in a rolling mode

Here, most of the particle mixing takes place in the active region and mixing in the passive region is negligible. The active layer particle mixing determines the surface renewal rate, which in turn affects the bed-freeboard heat and mass transfer and chemical reactions (Ding et al., 2001). The heat transfer is, however, not included in the present work, which focuses on the particle motion.

### 2.2 Governing Equation of Two-Fluid Model

#### 2.2.1 Continuity Equations

The continuity equations for the gas phase and the solid phase are as follows:

$$\frac{\partial}{\partial t}(\varepsilon_g \rho_g) + \nabla \cdot (\varepsilon_g \rho_g v_g) = 0 \quad (1)$$

$$\frac{\partial}{\partial t}(\varepsilon_s \rho_s) + \nabla \cdot (\varepsilon_s \rho_s v_s) = 0 \quad (2)$$

$$\varepsilon_g + \varepsilon_s = 1 \quad (3)$$

Here,  $\rho$  is density,  $v$  is velocity,  $\varepsilon$  is volume fraction and  $t$  is time.  $S$  and  $g$  refer to solid phase and gas phase, respectively.

#### 2.2.2 Momentum Equations

Momentum equations describe how the viscous, pressure and gravity forces govern the motion of the gas and the solid particles. The momentum equations for the gas phase and the solid phase are written as:

$$\frac{\partial}{\partial t}(\varepsilon_g \rho_g v_g) + \nabla \cdot (\varepsilon_g \rho_g v_g v_g) = -\varepsilon_g \nabla P_g + \varepsilon_g \rho_g g - \beta_{gs}(v_g - v_s) + \nabla \cdot (\varepsilon_g \tau_g) \quad (4)$$

$$\frac{\partial}{\partial t}(\varepsilon_s \rho_s v_s) + \nabla \cdot (\varepsilon_s \rho_s v_s v_s) = -\varepsilon_s \nabla P_g + \varepsilon_s \rho_s g - \beta_{gs}(v_g - v_s) + \nabla \tau_s \quad (5)$$

Here  $P_g$ ,  $g$ ,  $\beta_{gs}$  and  $\tau_g$  are the fluid pressure, gravity, drag coefficient between the gaseous and solid phases and viscous stress tensor of the gas phase, respectively.

The viscous stress tensor for the gas phase,  $\tau_g$  in Eq (4), and for the solid phase,  $\tau_s$  in Eq (5), are given by the Newtonian form:

$$\tau_g = \nu_g \left[ \nabla v_g + (\nabla v_g)^T - \frac{2}{3} \mu_g (\nabla \cdot v_g) I \right] \quad (6)$$

$$\tau_s = (-P_s + \zeta_s \nabla \cdot v_s) I + \mu_s \left\{ \left[ \nabla v_s + (\nabla v_s)^T \right] - \frac{2}{3} (\nabla \cdot v_s) I \right\} \quad (7)$$

Here  $P_s$ ,  $\mu_s$ ,  $\zeta_s$  and  $I$  are solid pressure, solid viscosity, solid bulk viscosity and unit tensor, respectively.

Particle-particle collisions create normal forces which are represented by the solid pressure  $P_s$  for one solid phase (Benyahia et al., 2000):

$$P_s = \varepsilon_s \rho_s \Theta + 2g_0 \rho_s \varepsilon_s^2 (1 + e_p) \Theta \quad (8)$$

Here,  $\Theta$  is the granular temperature (further explained below),  $g_0$  is the radial distribution function and  $e_p$  is the particle-particle restitution coefficient.

The bulk viscosity of the solid,  $\zeta_s$  in Eq (7), is given by (Neri and Gidaspow, 2000):

$$\zeta_s = \frac{4}{3} \varepsilon_s^2 \rho_s d_p g_0 (1 + e_p) \sqrt{\frac{\Theta}{\pi}} \quad (9)$$

Here,  $d_p$  is the particle diameter.

The solid shear viscosity in Eq (7) is given as (Arastoopour, 2001):

$$\mu_s = \frac{4}{5} \varepsilon_s^2 \rho_s d_p g_0 (1 + e_p) \sqrt{\frac{\Theta}{\pi}} + \frac{10 \rho_s d_p \sqrt{\pi \Theta}}{96 (1 + e_p) \varepsilon_s g_0} \left[ 1 + \frac{4}{5} \varepsilon_s g_0 (1 + e_p) \right]^2 \quad (10)$$

Wen and Ergun (Huilin and Gidaspow, 2003) proposed that the exchange coefficient  $\beta_{gs}$  between the gas and the solid phase given in Eq (4) and (5) could be calculated by:

$$\beta_{gs}|_{Wen \& Yu} = \frac{3}{4} C_D \frac{\rho_s \varepsilon_s |v_g - v_s|}{d_p} \varepsilon_g^{-2.65} \quad \varepsilon_g > 0.8 \quad (11)$$

$$\beta_{gs}|_{Ergun} = 150 \frac{(1 - \varepsilon_g) \varepsilon_s \mu_g}{(\varepsilon_g d_p)^2} + 1.75 \frac{\rho_s \varepsilon_s |v_g - v_s|}{\varepsilon_s d_p} \quad \varepsilon_g \leq 0.8 \quad (12)$$

The drag coefficient depends on the value of the Reynolds number, Re:

$$\begin{cases} C_D = \frac{24}{Re} (1 + 0.15 Re^{0.687}) & Re < 1000 \\ C_D = 0.44 & Re \geq 1000 \end{cases} \quad (13)$$

$$Re = \frac{\rho_g \varepsilon_g |v_g - v_s| d_p}{\mu_g} \quad (14)$$

### 2.2.3 Kinetic Theory of Granular Flow

Granular kinetic theory is extensively used in granular flow modelling to achieve a high level of accuracy of model results to be able to compare with data from the actual system. This theory considers the particle-particle collisions to predict physical properties of the particulate phase. The kinetic theory has been widely used in modelling of fluidized beds to model solid particles in a gas.

A new variable  $\theta$ , called the granular temperature, was introduced in this theory. It is a measure of the kinetic energy of the solid. Granular temperature is defined as one-third of the mean square velocity of the random motion of particles  $\theta = v_s^2/3$ , and  $v_s^2$  is the square of the fluctuating velocity of the particle. A transport equation for the granular temperature can be written as (Huilin et al., 2001):

$$\frac{3}{2} \left[ \frac{\partial}{\partial t} (\varepsilon_s \rho_s \theta) + \nabla \cdot (\varepsilon_s \rho_s \theta) v_s \right] = (\nabla P I + \varepsilon_s \nabla \tau_s) : \nabla v_s + \nabla \cdot (k_s \nabla \theta) - \gamma_s + \Phi_s + D_{gs} \quad (15)$$

Here,  $\gamma_s$  is dissipation of turbulent kinetic energy,  $\Phi_s$  is energy exchange between gas and particle and  $D_{gs}$  is energy dissipation.

The turbulent kinetic energy dissipation,  $\gamma_s$  in Eq (15), is given as (Neri and Gidaspow, 2000):

$$\gamma_s = 3(1 - e_p^2) \varepsilon_s^2 \rho_s g_0 \Theta \left( \frac{4}{d_p} \sqrt{\frac{\Theta}{\pi}} - \nabla \cdot v_s \right) \quad (16)$$

The radial distribution for one solid phase can be expressed as (Rahaman et al., 2003):

$$g_o = \left[ 1 - \left( \frac{\varepsilon_s}{\varepsilon_{s,max}} \right)^{1/3} \right]^{-1} \quad (17)$$

The energy exchange between the fluid and solid phases in Eq (15) is defined as (Huilin and Gidaspow, 2003):

$$\Phi_s = -3\beta_{gs}\Theta \quad (18)$$

The rate of energy dissipation per unit volume is in the form of the following equation:

$$D_{gs} = \frac{d_p \rho_s}{4\sqrt{\pi\Theta}} \left( \frac{18\mu_g}{d_p^2 \rho_s} \right)^2 |v_g - v_s|^2 \quad (19)$$

## 2.3 Simulation

The simulations were performed under rolling mode as this mode is considered to give good mixing. The rotational speed of the cylinder was maintained under a Froude number of  $16 \times 10^{-4}$  to achieve the rolling mode. The cylinder and the particles rotate in the counterclockwise direction.

### 2.3.1 Physical Properties of Materials and Model Parameters

In this study, two granular phases, made of  $\text{CaCO}_3$  and  $\text{Al}_2\text{O}_3$  were used in the simulations. Table 1 shows the related physical properties of gas and solids with model parameters.

**Table 1.** Physical Properties of Materials and Model Parameters

| Parameter   | Description             | Value |
|---|-------------------------|-------|
| $\rho_{\text{CaCO}_3}$ (kg/m <sup>3</sup> )         | Particle density        | 1760  |
| $\rho_{\text{Al}_2\text{O}_3}$ (kg/m <sup>3</sup> ) |                         | 3000  |
| $d_{\text{CaCO}_3}$ (μm)                            | Particle diameter       | 175   |
| $d_{\text{Al}_2\text{O}_3}$ (μm)                    |                         | 1000  |
| f (%)   | Degree of particle fill | 15    |
| $\omega$ (rpm)                                      | Rotational speed        | 2     |

### 2.3.2 Geometry and Mesh

A circle with 0.4m diameter was created in DesignModeler to represent the transverse plane of the rotating cylinder. A mesh was refined to yield about 5500 elements. Figure 2 provides the mesh of the transverse plane.

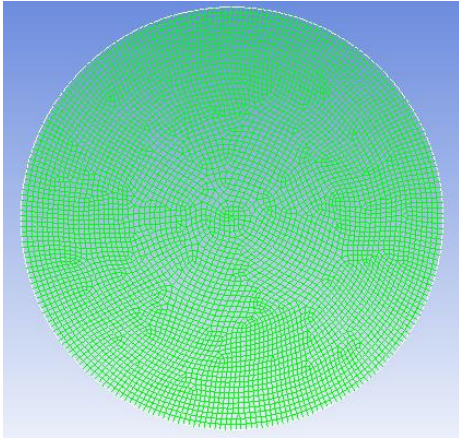


Figure 2. Mesh of the transverse plane

### 2.3.3 Initial and Boundary Conditions

The main boundary condition of the transverse plane in a rotating cylinder is the relative motion of the bed material and the rotating wall. There, a no-slip condition was assumed, meaning that the relative velocities of the gas and the particles at the wall are set to zero. And it was assumed that particles were subjected to wall friction and gravity.

### 2.3.4 Solution Strategy and Convergence Criteria

In this study, the finite volume approach was used to solve all the governing equations of the model. Since the flows could be considered incompressible, a pressure-based solver was used. The pressure-velocity coupling was done by a segregated algorithm called “SIMPLE” (Patankar and Spalding, 1972). A second order upwind scheme was used for discretization of the governing equations. The volume fraction was discretized according to the QUICK scheme (Versteeg and Malalasekera, 2007). The time step of the simulations was  $10^{-3}$  s and residual values for the convergence were set to  $10^{-3}$ .

## 3 Results and Discussion

### 3.1 Motion of a Single Solid Phase in a Transverse Plane

First, two simulations were performed to understand the bed behavior of  $\text{CaCO}_3$  and  $\text{Al}_2\text{O}_3$ , respectively. Figures 3(a) and (b) show the volume fraction contours of  $\text{CaCO}_3$  at 0s and pseudo-steady-state. Initially the top surface is flat, but with the time particles gradually move upwards, following the wall rotation. After a certain time period particles reach a maximum height and then roll down along the top layer in a continuous cyclic motion.

The results indicate that the bed material can be divided into two zones, one active and one passive region. In the active layer, particles move down with relatively high velocities compared to the passive layer.

Figure 4 illustrates the magnitude of the velocity field of  $\text{CaCO}_3$ . Two separated layers can be observed in that a thin upper layer moves with higher velocities than the thick lower layer. Figure 5 shows the velocity contours of  $\text{CaCO}_3$  particles, which also reveal that the active layer has much higher velocity magnitudes than the passive layer, and the zero velocity region is clearly observed.

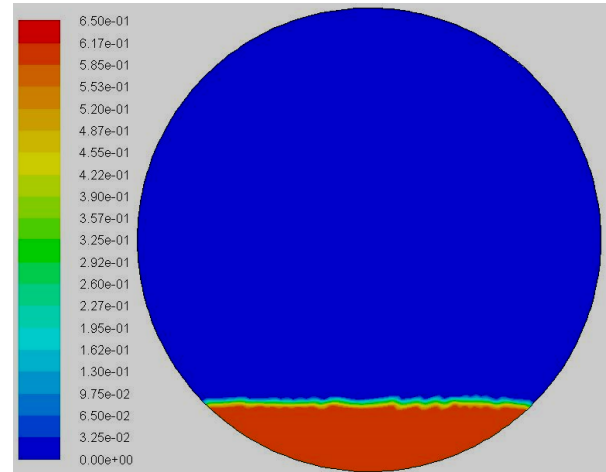


Figure 3(a). Volume fraction contours of  $\text{CaCO}_3$

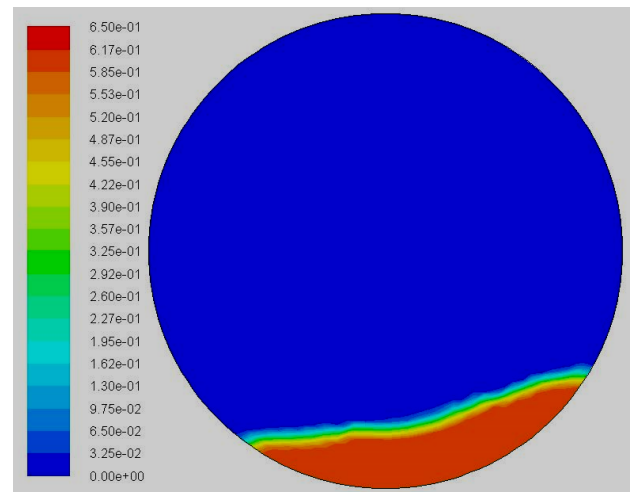


Figure 3(b). Volume fraction contours of  $\text{CaCO}_3$

In general, the downwards motion in the left direction in the active layer balances the upwards motion in the right direction in the bottom layer, resulting in cyclic pseudo-steady-state flow process. This means that top layer particles exposed to heat transfer from above, as is the case in rotary kilns, would mix with particles in the bottom layer and transfer heat by conduction.

Very similar results were found for the  $\text{Al}_2\text{O}_3$  motion, so no graphics are included for this particle type.

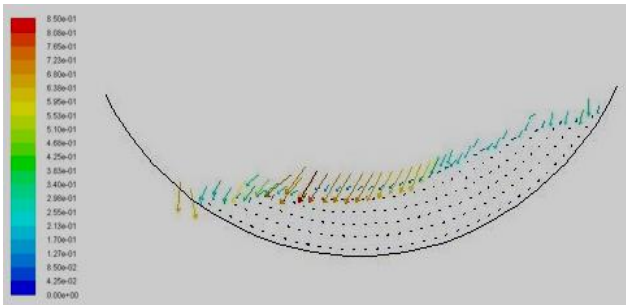


Figure 4. Velocity vector of particle at pseudo-steady-state

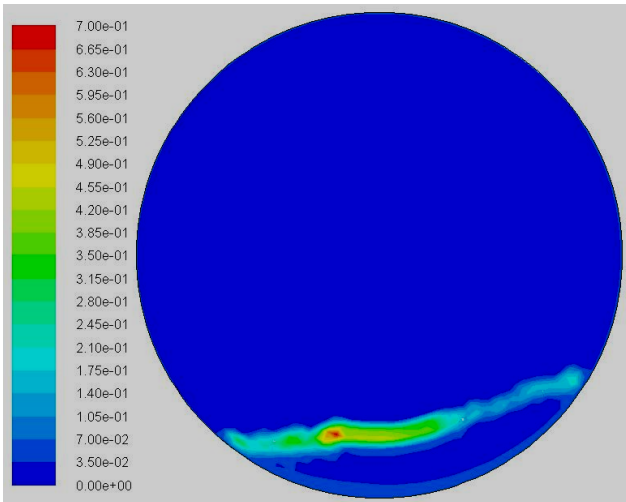


Figure 5. Velocity contours of CaCO<sub>3</sub> at pseudo-steady-state

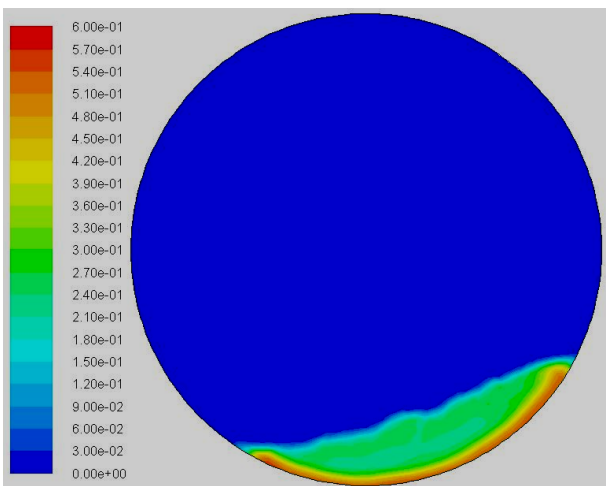


Figure 6. Volume fraction contours of Al<sub>2</sub>O<sub>3</sub> in the mixture at pseudo-steady-state

### 3.2 Mixing of Two Solid Phases in a Transverse Plane

A mixture of CaCO<sub>3</sub> and Al<sub>2</sub>O<sub>3</sub> were simulated to investigate the mixing performance when two solids with different characteristics are exposed to the rotational motion. Volume fractions of both solids were examined to understand the mixing behavior. Contour plots of volume fractions of solids are shown in Figures 6 and 7. Figure 6 shows the volume fraction variation of

Al<sub>2</sub>O<sub>3</sub> in the particle bed, revealing that Al<sub>2</sub>O<sub>3</sub> accumulates at the bottom of the particle bed. CaCO<sub>3</sub>, as seen in Figure 7, is collected in the middle of the bed. This illustrates that a mixture of two particle types will undergo segregation instead of mixing during rotation.

Variation of particle size and density are the key factors of segregation in a rotating cylinder. In the active layer of the particle mixture, both solids roll down relative to the slowly moving passive layer. Due to this particle motion, small particles have a higher probability to separate within the active layer and move into middle of the bed. Larger and denser particles move downwards by sustaining the active layer and entering into the passive region at the bottom of the particle bed, near to the wall.

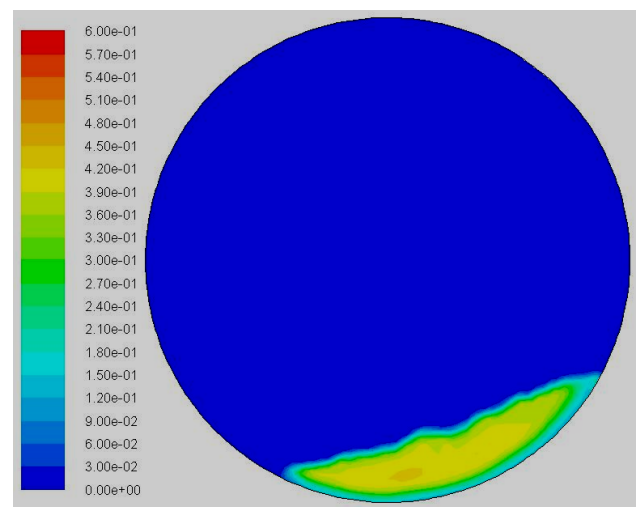


Figure 7. Volume fraction contours of CaCO<sub>3</sub> in mixture at pseudo-steady-state

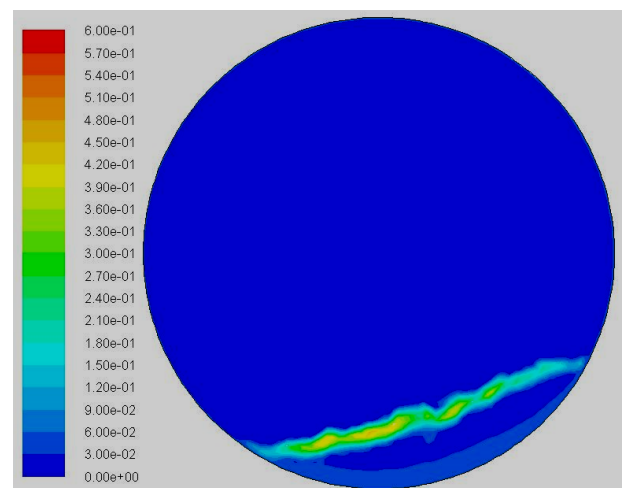
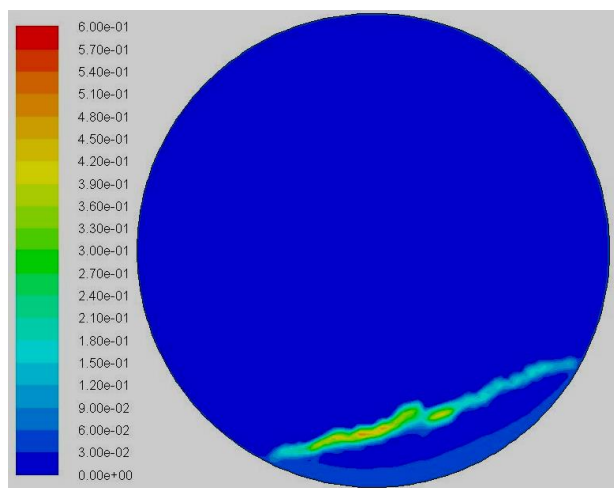


Figure 8. Velocity contours of Al<sub>2</sub>O<sub>3</sub> in mixture at pseudo-steady-state



**Figure 9.** Velocity contours of  $\text{CaCO}_3$  in mixture at pseudo-steady-state

Velocity contours of both solids are shown in Figure 8 and 9. Both materials are present in the active layer of the mixing bed. The simulation results depict that the intensity of the velocity contours decrease in  $\text{CaCO}_3$  rather than in  $\text{Al}_2\text{O}_3$  when materials move towards the lower (left) end of the active layer. This indicates that a smaller amount of  $\text{CaCO}_3$  particles will remain at the active layer lower end due to segregation.

Generally, particles start to segregate when they are subjected to motion. The particle motion in the active layer facilitates segregation of particles of different size and density.

## 4 Conclusions

Mathematical modelling of a two-dimensional transverse plane in rotating cylinder, based on the Eulerian approach and the kinetic theory of granular flows, predict the particles mixing behavior in a rotary kiln. The rolling mode can be recommended to achieve internal mixing for a single solid phase. However, particle segregation is observed when two different granular phases are being exposed to the rotary motion under the rolling mode. Lighter and smaller particles are collected in the middle section of the bed while particles with a higher density and size get collected at the bottom of the rotating cylinder. More studies need to be done to understand the mixing mechanism for two granular particles under the rolling mode. In addition to that, further studies are required to determine the best mode for the particles motion in rotating cylinder. Some industrial applications use internal lifters to acquire a higher degree of material mixing. 2-D simulation of the transverse plane with lifters attached to the wall may be applied to investigate to what extent this will improve mixing efficiency of two granular phases.

## References

- H. Arastoopour. Numerical simulation and experimental analysis of gas/solid flow systems: 1999 Fluor-Daniel Plenary lecture. *Powder Technology*, 119: 59-67, 2001.
- S. Benyahia, H. Arastoopour, T. M. Knowlton, and H. Massah. Simulation of particles and gas flow behavior in the riser section of a circulating fluidized bed using the kinetic theory approach for the particulate phase. *Powder Technology*, 112: 24-33, 2000.
- A. A. Boateng, *Rotary Kilns: Transport Phenomena and Transport Processes*. USA: Butterworth-Heinemann publications, 2008.
- C. Crowe, M. Sommerfeld, and Y. Tsuji, *Multiphase flows with droplets and particles*. USA: CRC Press LLC, 1998.
- Y. Demagh, Hocine, B. Moussa, M. Lachi, and L. Bordja. Surface particle motion in rotating cylinders: Validation and similarity for an industrial scale kiln. *Powder Technology*, 224: 260-272, 2012.
- Y. L. Ding, J. P. K. Seville, R. Forster, and D. J. Parker. Solid motion in rolling mode rotating drums operated at low to medium rotational speeds. *Chemical Engineering Science*, 56: 1769-1780, 2001.
- L. Huilin and D. Gidaspow. Hydrodynamics of binary fluidization in a riser: CFD simulation using two granular temperatures. *Chemical Engineering Science*, 58: 3777-3792, 2003.
- L. Huilin, D. Gidaspow, and E. Manger. Kinetic theory of fluidized binary granular mixtures. *Phys. Rev. E*, 64: 061301: 1-8, 2001.
- H. Liu, H. Yin, M. Zhang, M. Xie, and X. Xi. Numerical simulation of particle motion and heat transfer in a rotary kiln. *Powder Technology*, 287: 239-247, 2016.
- A. Neri and D. Gidaspow. Riser hydrodynamics: Simulation using kinetic theory. *AIChE Journal*, 46: 52-67, 2000.
- S. V. Patankar and D. B. Spalding. A calculation procedure for heat, mass and momentum transfer in three-dimensional parabolic flows. *International Journal of Heat and Mass Transfer*, 15: 1787-1806, 1972.
- M. F. Rahaman, J. Naser, and P. J. Witt. An unequal granular temperature kinetic theory: description of granular flow with multiple particle classes. *Powder Technology*, 138: 82-92, 2003.
- M. A. R. Valle. *Numerical Modelling of Granular Beds in Rotary Kilns*. Master of Science in Computer Simulations for Science and Engineering, Department of Applied Mathematical Analysis, Delft University of Technology, 2012.

H. K. Versteeg and W. Malalasekera, *An introduction to computational fluid dynamics*, second ed. England: Pearson Education Limited 2007.

H. Yin, M. Zhang, and H. Liu. Numerical simulation of three-dimensional unsteady granular flows in rotary kiln. *Powder Technology*, 253: 138-145, 2014.